Numerical simulation of VIV of a elastic mounted cylinder with low mass-ratio

Xu Junling [1] and Zhu Ren-qing [2]

[1] Jiangsu university of science and technology, Zhen jiang , China,212003
E-mail: viv.1980@163.com

[2] Jiangsu university of science and technology, Zhen jiang , China,212003
E-mail: zjcyzrq@hotmail.com

Abstract

Recently with the development of international offshore oil industry to deep water, the vortex-induced vibrations (VIV) of deep riser are paid more and more attention to by many researchers. In the present work, Reynolds - averaged Navier – Stokes (RANS) equations are combined with SST $\kappa-\omega$ turbulent model to simulate the stream-wise and transverse movement of the elastic mounted cylinder with natural frequency ratio $f_x / f_y = 1$ and low mass-ratio, and the Re number is chosen from 5300 to 32000. Then the four-order Runge - Kutta Method is applied in the solution of oscillating equations of cylinder. Then, compared with recent experimental results, the relation between reduced velocity and parameter of cylinder which include the lift coefficient, the drag coefficient, displacement and the vortex structure are discussed in detail. In the present numerical simulation, the lock-in phenomenon, the hysteretic phenomenon and beating behavior are reproduced which have been observed in the experiments.

Keywords: VIV;lowmass-ratio; stream-wise and transverse motion; lock-in; beating; vortex shedding model; CFD

Introduction

With oil exploration to extend deeper waters, marine infusion pipeline design requirements become more and more high, In order to explore the damage of deep riser by vortex-induced vibration caused by wave and current, the researchers conducted a lot of research work.

Early the study on the vortex-induced vibration was based on high mass-ratio, because the stream-wise vibrations amplitude is small Relatively, under the high mass ratio, the influence of stream-wise oscillations on transverse oscillations is very small. Thus in generally speaking, on the early experiments Restrict stream-wise motion should be used. With the mass-ratio declining, the influence of stream-wise oscillations on transverse oscillations is become more and more obvious. In the case of Moe & Wu(1990),the mass ratios were very different in the two directions ,and the natural frequency ratio was set to $f_x / f_y = 2.18$. Under these special conditions, they find a broad regime of velocity U^* over which resonant amplitudes are found (with transverse normalized amplitude close to $A_Y^* = A/D = 1$), but no evidence of distinct response branches. Later experiments of Aarpkaya (1995) have concentrated on varius ratios between f_x and f_y, although he shows one set of amplitude data for XY-motion where $f_x = f_y$,indicating a slight increase in transverse amplitude and a shift to higher U^* for the peak transverse response, when compared with the Y motion case. A comprehensive study on the response of a rigid, elastically mounted cylinder in two degrees of freedom (2-dof) was presented by Jauvtis and Williamson (2004), with equivalent mass ratios and natural frequencies in both directions and a low structural damping. For ($m^* = 1.04$), however, the system response was drastically modified: the upper branch was replaced by a new response branch (denoted ‘super-upper’) characterized by different vortex dynamics which is 2T model. The experiment of elastically mounted cylinder in two degrees of freedom with more high Re and more low mass-ratio was presented by Sanchis, Sælevik Grue[6](2006). As experiment was restricted by the conditions, testing reduced velocity was only completed between 4.5 and 6.9, and obtained max amplitude was 1.1.

Recently with the extensive application of CFD, Numerical simulation of cylinder VIV is adopted by more and more people. In this work, Finite Volume Method is combined with appropriate turbulent model to simulate the 2D elastic mounted cylinder VIV under condition of uniform inflow.

In this paper, in conjunction with experiment results of Sanchis, Sælevik and Grue[6], the problems should be analyzed in detail which is how many the transverse amplitude can be , how much the influence of stream vibration on wake field should be and whether the 2T model of vortex structure under peak transverse amplitude appears or not.

1 Numerical calculation model

It is assumed that circular cylinder is mounted as a spring-damper-mass system as shown in Fig.1a. In the uniform inflow, the dynamic equation of oscillate cylinder can described by

$$m\ddot{x} + c\dot{x} + kx = F_x(t) \quad (1)$$

$$m\ddot{y} + c\dot{y} + ky = F_y(t) \quad (2)$$

where m is the mass per unit length of the cylinder; c is the structural damping; k ,the spring constant; $F_x(t)$ is drag of the cylinder , $F_y(t)$ is lift of the cylinder. The variables of Eq (1) are normalized as:

$$F_x = \frac{1}{2C_d \rho_f U^2 D} \ , \ X = \frac{x}{D} \ , \ \tau = \frac{tU}{D} \ , \ \frac{dx}{dt} = U\frac{dX}{d\tau} \ ,$$

$$\frac{d^2x}{dt^2} = \frac{U^2}{D}\frac{dX}{d\tau} \ , U_r = \frac{U}{f_n D} \ \ m^* = \frac{4m}{\rho\pi D^2} \ , \zeta = \frac{c}{2\sqrt{km}} \ ,$$

$$f_n = \frac{1}{2\pi}\sqrt{\frac{k}{m}}$$

then ,the nondimensional vibration equation along the flow direction for the cylinder can be written as:

$$\frac{d^2X}{d\tau^2} + \frac{4\pi\zeta}{U_r}\frac{dX}{d\tau} + \frac{4\pi^2}{U_r^{\ 2}}X = \frac{2C_d}{\pi m^*} \tag{3}$$

where U is the velocity of flow fluid, D is the cylinder diameter, C_d is drag coefficient, ρ_f is density of fluid, ρ is the density of cylinder, and f_n is the natural frequency of cylinder.

According to the same method, the equation of oscillation through transverse direction can be written as:

$$\frac{d^2Y}{d\tau^2} + \frac{4\pi\zeta}{U_r}\frac{dY}{d\tau} + \frac{4\pi^2}{U_r^{\ 2}}Y = \frac{2C_l}{\pi m^*} \tag{4}$$

In this papers, in order to be agree with the experiments, noted $U^* = U / f_{wtr} D$, where f_{wtr} is the frequency of cylinder in the water.

The fluid force can be assumed to be a constant at the arbitrary small time step, and is solved by Reynolds-averaged Navier-Stokes(RANS) equations. Then the four-order Runge-Kutta Method is applied in the solution of oscillating equations of cylinder.

When oscillate amplitude and oscillate frequency are steady, the corresponding displacement of cylinder can be approximately regard as

$$y = A\sin(\omega_{ex} t) \tag{5}$$

in which A is the max amplitude of vibration and ω_{ex} is oscillation frequency. Assuming the vortex shedding is "lock" on to the vibration frequency of the cylinder, the linearized lift force can be expressed as

$$C_y = C_L \sin(\omega_{ex} t + \phi) \tag{6}$$

where C_L is the max of lift coefficient, ϕ is the phase angle between the fluid force and the body displacement. In a self-excited case, it will be a positive value indicating that the fluid force leads to the motion of the cylinder. In comparison, it can be a negative value in the forced vibration with energy transferring from the structure to the fluid.

The lift force can be divided into two parts as:

$$C_y = C_{Lv}\cos(\omega_{ex} t) + C_{La}[-\sin(\omega_{ex} t)] \tag{7}$$

where C_{Lv} is the drag component in phase with velocity and C_{La} is the inertia component in phase with acceleration.

The comparison between Eq(6) and Eq(7) leads to

$$C_{Lv} = C_L \sin\phi \tag{8}$$

$$C_{La} = -C_L \cos\phi \tag{9}$$

The Eq(4) can be deduced and forms

$$\ddot{Y} + 2\zeta\dot{Y} + Y = \frac{C_y \rho_f U^2}{2\omega_n^2 m} \tag{10}$$

in which, ζ is the damping ratio and ω_n is actual oscillate frequency of cylinder. Introduce Eq(5) and Eq(6) into Eq(8) can be obtained:

$$\frac{A}{D} = \frac{1}{4}\frac{C_{Lv}}{\pi^3 m^* \zeta}\frac{f_n}{f_{ex}}\left(\frac{U}{f_n D}\right)^2 \tag{11}$$

$$\frac{f_{ex}}{f_n} = \left[1 + \frac{1}{2}\frac{C_{La}}{\pi^3 m^*}\frac{A}{D}\left(\frac{U}{f_n D}\right)^2\right]^{1/2} \tag{12}$$

The components of linearized transverse fluid force C_{Lv} and C_{La} are deduced from Eq(11) and Eq(12)

$$C_{Lv} = 4\pi^3 m^* \zeta \frac{A}{D}\frac{f_{ez}}{f_n}\left(\frac{f_n D}{U}\right)^2 \tag{13}$$

$$C_{La} = 2\left[\left(\frac{f_{ex}}{f_n}\right)^2 - 1\right]\pi^3 m^* \frac{A}{D}\left(\frac{f_n D}{U}\right)^2 \tag{14}$$

The phase angle between fluid force and motion can be obtained by Eq(8) and Eq(9)

$$\varphi = \arctan\left(-C_{Lv} / C_{La}\right) \tag{15}$$

2 ploting and testing with mesh

In this paper, the radius of cylinder is D, and the whole flow domain is a square, which is 40*D length and 30*D width. The distance of the upstream is 15 times than the radius of the cylinder. i.e. 15*D, and the length of downstream is 25*D. In the fluid domain, the direction of flow is specified from left to right. In the numerical calculation, as the initial grid the mixed unstructured mesh is applied, which includes the structure quadrilateral mesh in the area of 2*D distance from the cylinder and triangular mesh in any other place. And the dynamic mesh method which includes spring based smoothing and local remeshing is adopted to deal with the unsteady moving boundary problem, in order to improve the quality of grid, the area in which the distance is 6*D is moving with the cylinder(see the Figure 1-b). In the present work, the Reynolds-averaged Navier-Stokes (RANS) equations are combined with corresponding turbulent model, and the Re number is chosen from 5300 to 32000. The grid of first

layer near cylinder Δy should be evaluated by the following eq (16), which need to satisfy $y^+ \approx 1$,

$$y^+ = 0.172 \frac{\Delta y}{D} R_e^{0.9} \quad (16)$$

In order to choose the suitable mesh for the consideration on the calculation precision and speed, here the test case of self-exciting oscillation response of SST $k-\omega$ turbulent model with $U^* = 4.5$ should be used to test three different meshes for the optimal selection. As shown in figure 1b, and the influence on the calculation results is presented in table 1. Through comparing of the above case, case b is used in this paper, which is the most reasonable in computing time and precision.

case	*a*	*b*	**c**
cell (single)	13683	19426	24549
time (hour)	11.6	15.2	18.3
Max in-line amplitude	0.188	0.195	0.196
Max transverse amplitude	0.890	0.971	0.971
Max lift coefficient	2.772	2.953	2.955
Max drag coefficient	3.243	3.588	3.590

Table 1 the results of three type mesh

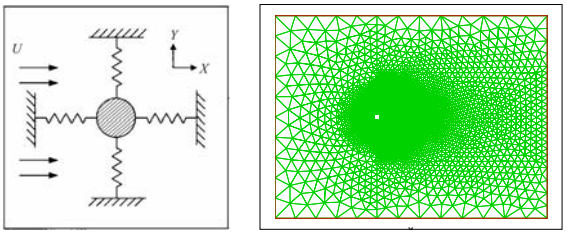

a vibrating model **b** computation model

Figure 1

3 results and discussion

In this paper, according to the experiment (A. Sanchis, G. Sælevik, J. Grue2006[6]) of elastic mounted cylinder with low mass ratio, the calculation parameters are chosen as follow, cylinder diameter D=0.08m, mass ratio $m^* = 1.04$, damping ratio $\zeta = 0.046$, frequency of oscillate in water $f_{wtr} = 0.42$, natural frequency ratio $f_x / f_y = 1$, and the Re number is from 5300 to 32000.

For convenient discussion, in this paper, the zone before $U^* = 4.5$ is defined as the initial branch, $U^* = 4.5 - 6.1$ is defined interim branch, $U^* = 6.1 - 10$ is defined lock-in branch, and $U^* = 10$ is defined low branch.

3.1 Analyse of trajectory shapes

Firstly, the comparison study of the trajectory shapes of cylinder between present work and experiment of Jauvtis & Williamson2004[4], in order to verify reliability of model. Figure2-a is the experiment of Jauvtis & Williamson2004 [4], and Figure2-b is the present work, in which respectively correspond initial branch, interim branch, the peak of amplitude, and lock-in branch. Through comparing, it is basically tallies that trajectory shapes between present work and experiment in corresponding area. So this model is reliable in the trajectory shapes.

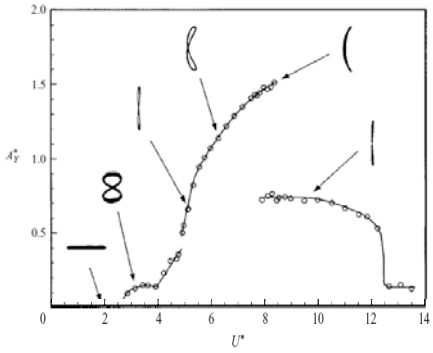

a X,Y trajectory shapes given by J & W(2004)

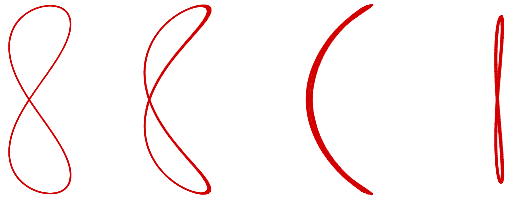

initial branch | interim branch | Peak of amplitude | Lock-in branch

b X,Y trajectory shapes in present work

figure2 trajectory shapes of cylinder in different branch

3.2 Analysis on Amplitude

Figure3(a) and (b),respectively shown that Amplitude of motion in the transverse and horizontal directions response on reduced velocity. In order to compare become clearing, the results of experiments of Jauvtis & Williamson2004[4] and A. Sanchis, G. Sælevik, J. Grue2006[6] are drew on the Figure3. Two response of amplitude are shown by Khalak&Williamson1999[5] in Figure 4, in which a is represent response of low $m^*\zeta$ （0.013） and b is represent response of high $m^*\zeta$ (0.255). In this papers, $m^*\zeta = 0.114$ is more close to 0.255 represent by Figure4-b than Figure4-a. comparing with figure3-a and figure4-b, , in this papers, have same tendency on response of the max transverse, comparison of experiment. And response of transverse amplitude of cylinder are considerly divided 2 branch, initial excitation branch(also defined initial up combined branch), and low branch.

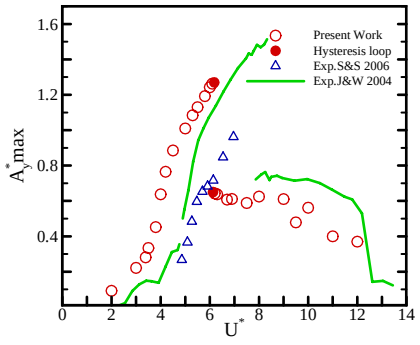

a max of transverse amplitude

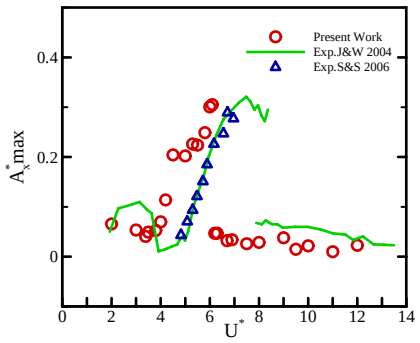

b max of stream-wise amplitude

Figure 3 max of transverse amplitude A_y^* and max of stream-wise amplitude A_x^* under different reduced velocity compared with experiment's results

In the steady flow velocity, the max transverse amplitude occur in $U^* = 6.15$, its value approach to 1,26, when around $U^* = 6.15$, transverse amplitude occur jump reduce phenomenon, which decreased to 0.6, and oscillation from interim branch into lock-in branch. In the experiment ,the hysteretic phenomenon between initial branch and low branch, which also recurrence in this Numerical simulation. Around $U^* = 6.1$, initial conditions of increased flow velocity and decreased flow velocity can lead to different result. When increased velocity, response of amplitude on jumping small amplitude is occur at $U^* = 6.18$, and when decreased velocity, which occur at $U^* = 6.12$. In the figure3-a,soid circle corresponding to the hysteretic of figure4-b.

In the experiment, the beating phenomenon is occurred at low reduced velocity in hysteretic domain, and similar conclusion also can be obtained from numerical simulation. The figure5-a is transverse motion of cylinder duration curve, in which transverse axis is dimensionless time t/T_n (T_n is cycle of fixed cylinder), vertical axis is dimensionless amplitude($A_y = y/D$). Show as figure5-a, the peak of oscillate change between two parallel lines, and do not fixed in a exact value. When $U_r \geq 6.2$, system into lock-in branch, vibration model of cylinder change from beating model into single frequency model, shown as figure5-b, vibration curve is approximated as sine curve. Then with increasing flow velocity, when $U^* \geq 10$, dimensionless amplitude is obviously decreased to about 0.36, oscillation of cylinder is divorced from lock-in domain.

Stream-wise amplitude is corresponding to transverse amplitude, shown as figure3-b, amplitude also divided into two branch, one is corresponding to initial branch of transverse oscillation, another is corresponding to low branch of transverse oscillation. In the initial branch, status of stream-wise amplitude transit gradually from small oscillation to big oscillation, when around $U^* = 6.1$, dimensionless amplitude reached the max value 0.3, and also occurred jump reduce. Entering lock-in branch, amplitude is maintain about 0.03.

It is noteworthy that the equilibrium position of stream-wise oscillation is not always offset from initial equilibrium position with increasing of U^*. From figure6' curve can found that, in the initial branch , equilibrium position of stream-wise oscillation is gradually offset from initial equilibrium position, when $U^* = 6.1$, dimensionless distance reach to 0.892. After entering lock-in branch, the equilibrium position of stream-wise oscillation is closed to initial equilibrium position with U^* increasing, when $U^* = 6.9$ the value is 0.577. With increasing of velocity, the effect of fluid flow to stream-wise oscillation is become more obviously, so the equilibrium position of stream-wise oscillation is offset from initial equilibrium position continuously.

3.3 The analysis of frequency

The figure 7 shows that the relations between the cross oscillation frequency and fixed average velocity, where f^* denotes the ratio between practical vibration frequency f_{ex} and fixed frequency f_{wtr}. In the outside of

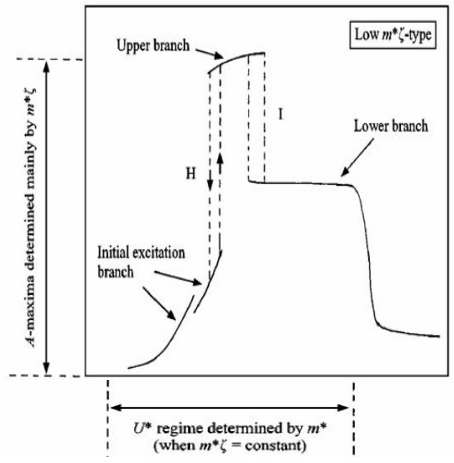

a max of transverse amplitude

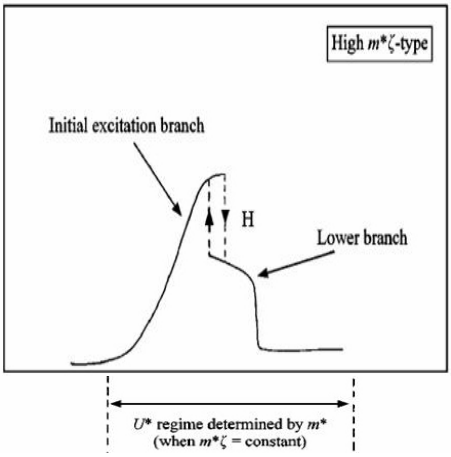

b max of stream-wise amplitude

Figure 4 The two distinct types of amplitude response (Vertical axes represent A^* and horizontal axes represent U^*), mode transitions are either hysteretic (H) or intermittently switching modes (I). (Khalak & Williamson, 1999)

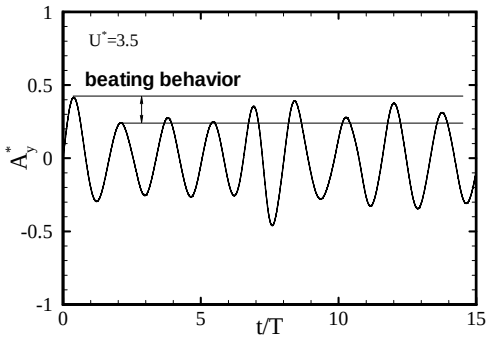

a beating behavior graph

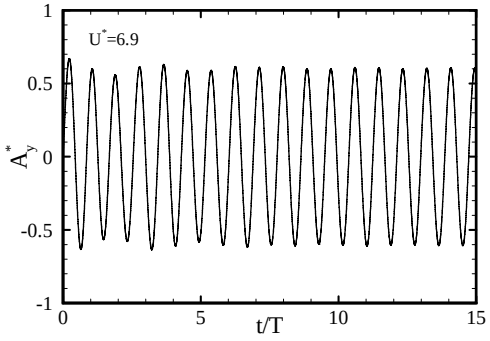

b single frequency model graph

Figure 5

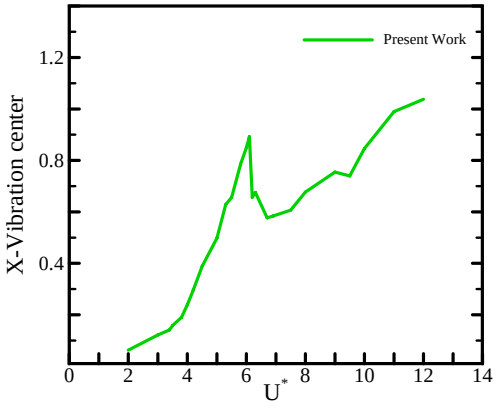

Figure 6 the equilibrium position of stream-wise oscillation

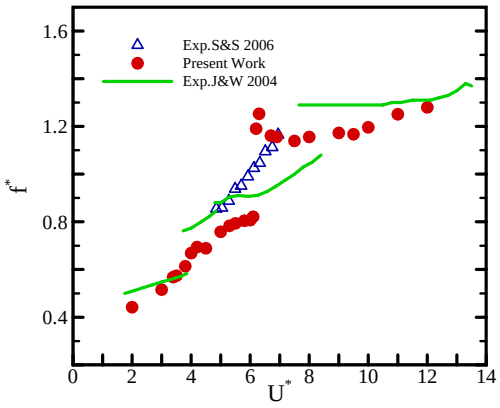

Figure 7 frequency response with reduced velocity

locking in zone, f_{ex} is basically equal to vortex frequency f_{st} of fixed cylinder (Strouhal frequency). In the locking in zone the frequency is locked near 1.155, in the experiment the corresponding f^* in the upper branch is about 1.3. When the reduced velocity goes on increasing to $U^* = 10$, the vibration frequency of cylinder is 1.273 and

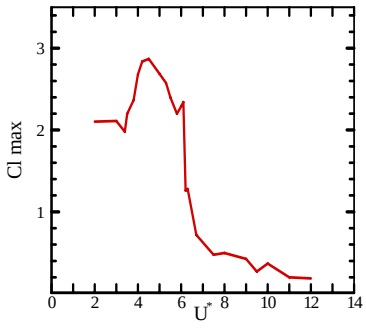

a max lift coefficient response with reduced velocity

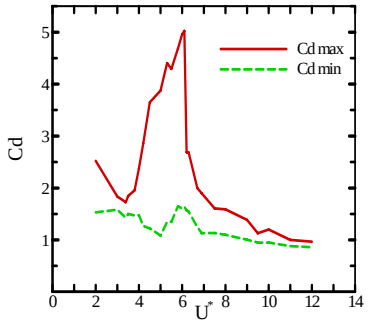

b max and min drag coefficient response with reduced velocity

Figure 8

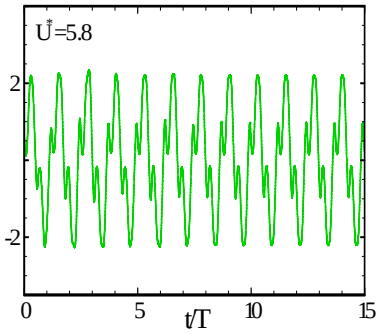

a beating phenomenon of lift

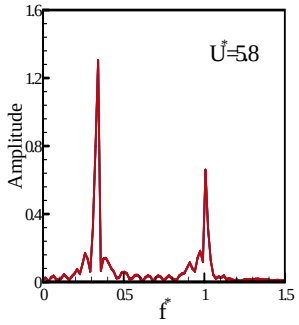

b lift spectrum analysis

Figure 9

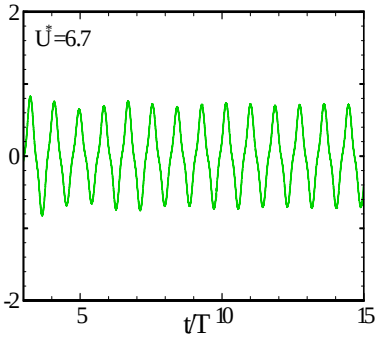

a single frequency of lift

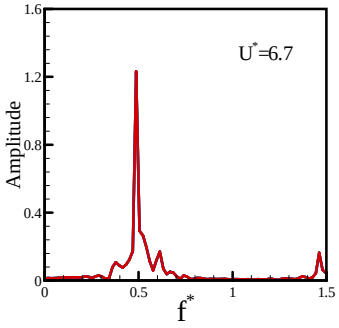

b lift spectrum analysis

Figure 10

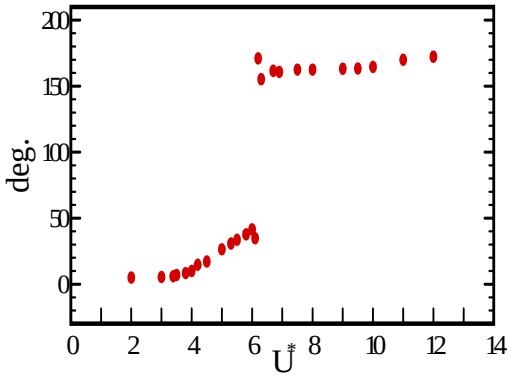

a phrase angle between lift and transverse motion

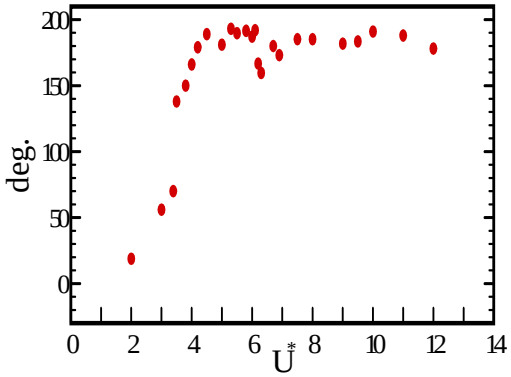

b phrase angle between drag and stream-wise motion

Figure 11

returns to nearby f_{st} again, which represents the end of locking in zone.

The in-line oscillation frequency is always about $2f_{ex}$, and is similar to the cross vibrate frequency.

3.4 The analysis of hydrodynamic

On the zone of initial branch, the cross amplitude is not obvious and the vibration frequency of lift is controlled by the vortex frequency f_{st} of fixed cylinder. With the increase of U^*, the lift amplitude increases step by step. It is noted that the maximum lift efficient does not appear on the transverse maximum amplitude and will be up to 2.87

at the $U^* = 4.5$ which denotes the entry of transition zone in figure 8-a. After in the transition zone, the lift coefficient gradually decreases and shows the instability and obvious beat phenomenon as shown in 9-a. Then the lift is translated by means of FFT transform and from the calculated data the lift is controlled by two frequencies (shown in figure 9-b). When $U^* \geq 6.2$, the system is the locking in state in figure 10-a,which presents the single frequency vibration, the lift is controlled by one frequency through the transform FFT to lift as shown in 10-b. When the fluid velocity continues to increase to $U^* = 11$, the lift amplitude reduces obviously, and keeps away from the locking in zone, and the force and oscillation of cylinder are controlled by two frequency.

In the figure 8-b, when the system is steady, the drag coefficient curves are plotted under different average velocity. Different from the lift, the maximum drag coefficient, which is about 5, appears at the state of $U^* = 6.1$ near the separation point between transition zone and locking in zone. But the value of drag coefficient decrease to 2.69 rapidly after the velocity is into the locking-in zone. The figure 8-b shows that the oscillation amplitude of drag coefficient is reflected in the zone between two curves. The oscillation amplitude is very small in the initial branch, but increases very quickly in the transition zone and is up to the maximum at the separate point between transition zone and locking in zone. At last in the locking in zone the amplitude turns to 0.56 and trends to a very small number with the increase of velocity.

3.5 The analysis of wake vortex

The phase angle φ between drag and in-line displacement changes from 0 to π degree and finishes in the initial branch. As shown in figure 11(b). The phase angle between lift and cross displacement, which changes from 0 to π in the transition zone, does not change obviously in the initial branch and transition zone (see figure 11). The variation of phase should lead to the switch and transformation of the vortex time and wake vortex. When the in-line oscillation is limited, 2S（two single

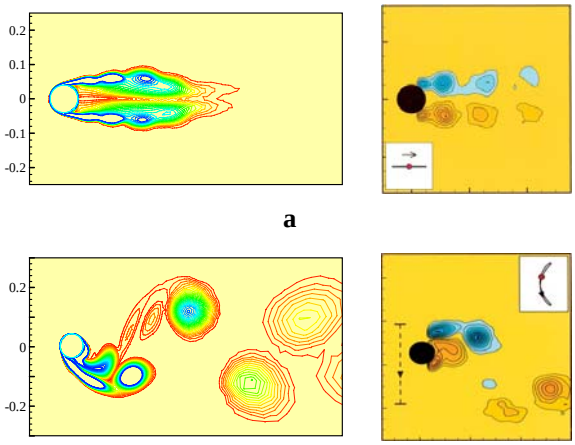

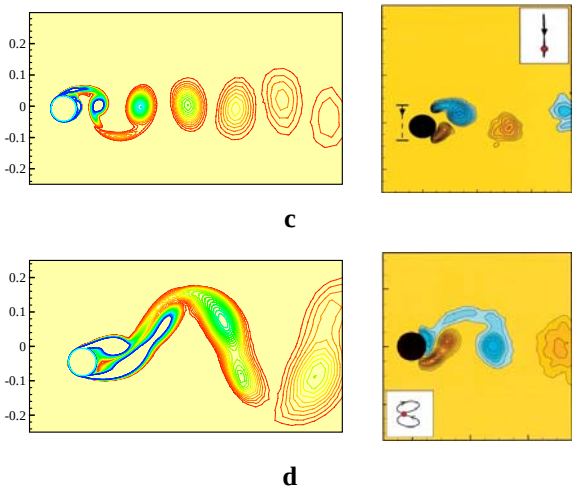

Figure 12 vortex shedding model compare with different branch

vortices shed per cycle） is discovered in the experiment, and wake vortex 2P model（two pair vortices shed per cycle ）appears. If the in-line oscillation is taken into account, in the experiment of Jauvtis & Williamson2004[4], SS （Stream-wise symmetric vortices shed per cycle ） model and wake vortex 2T（two trip lets of vortices per cycle）model are founded. In the this numerical case, the above wake vortex is well represented again.

In the figure 12, the left figure is the numerical simulation of this article, and the right figure is the experimental results of Jauvtis & Williamson2004[4]. As shown in figure 12, when the cylinder is at the original phase of initial branch, the in-line amplitude plays a dominant role and the wake vortex is SS model in which a pair of parallel vortices is formed at each period. With the increase of fluid velocity, the cross amplitude of cylinder is not large, but if the cross amplitude is larger than the in-line amplitude, the wake vortex will change to 2S model which is presented in the approximate form of Karman vortex street (see the figure 12(b)). When the amplitude is up to the maximum, the 2T model appears and at each period two groups of vortex are formed. Every group includes three vortices in which two vortices are the same rotation direction and the other is counter which is a far lower than two other vortices as shown in figure 12(c). In the locking in zone, the wake vortex exists in 2P model in which at each period two pairs of counter rotation vortices are formed. On the side of low U^* of locking in zone, the difference of swirling strength is relative large and with the lapse of time the small vortices dissipate in the fluid, the wake flow is 2S model. On the side of high U^*, the strength of a pair of vortices is relative same, the wake flow is basically 2P model as shown in 12(d).

4 Conclusions

1 Under the high $m^*\zeta$, the motion of cylinder is only two categorizations. The one is initial excited branch which is also called the combined branch between the initial and upper part, in this branch the maximum amplitude will appear. And the other is the inferior branch, on the side of low U^* the locking in will occur, the hysteretic loop exists between the initial and the inferior branch, and on the side of low U^* of hysteretic loop the beat oscillation will happen.

2 After coming into the zone of locking in, the balance position of in-line oscillation will be close to the initial equilibrium position. Further, when the influence of fluid velocity becomes stronger, the vibration center will go on keeping away from the initial balance position.

3 When the initial branch just flows into the transition zone, the lift is up to the maximum. With the development of the initial branch in the transition zone the lift is turn down slowly, but the cross amplitude increases step by step.

4 When the track is at the initial branch, the influence of in-line oscillation is obvious, and a SS wake vortex model appears. But on the position of maximum amplitude the 2T wake vortex appears.

6 The phenomenon (locking in, hysteresis and beat oscillation) in experiment is well represented by the present numerical simulation.

References

[1] Wu G A,Moe Z J. The lift force on a cylinder vibrating in a current [J].Journal of Offshore Mechanics and Arctic Engineering.112: 297-303. 1990

[2] Sarpkaya T. Hydrodynamic damping flow-induced oscillations and biharmonic response[J]. ASME Journal of Offshore Mechanics and Arctic Engineering.117:232-238. 1995

[3] Jauvtis N, Williamson CHK. Vorte-inducedvibration of a cylinder with two degrees of freedom[J]. Journal of Fluids and Structures. 17:1035-1042. 2003

[4] Jauvtis N, Williamson CHK.The effect of two degrees of freedom on vertex-induced vibration at low mass and damping[J]. Journal of Fluids Mechanics 509:23-6.22004

[5] Khalak, A., Williamson, C.H.K. Motions. forces and mode transitions in vortex-induced vibrations at low mass-damping. Journal of Fluids and Structures 13, 813-851. 1999

[6]A Sanchis, G Sælevik,J Grue[J]. Journal of Fluids and Structures. 1:1-13. 2008

[7]Al-Jamal, H. and Dalton, C.. Vortex induced vibrations using large eddy simulation at a moderate Reynolds number[J]. Journal of Fluids and Structures 19, 73-92. 2004

[8]Carberry, J., Govardhan, R, Sheridan, J, Rockwell, D and Williamson, C.H.K. Wake states and response branches of forced and freely oscillating cylinders[J]. European Journal of Mechanics - B/Fluids 23, 89-97. 2004

[9]郭海燕 傅强 娄敏. 海洋输液立管涡激振动响应及其疲劳寿命研究[J]. 工程力学 22(4):220-224. 2005

[10]Balasubramanian S,Skop R A.A nonlinear oscillator model for vortex shedding from cylinders and cones in uniform and shear flows[J].Journal of Fluids and Structures,.10:197-214. 1996

[11]Sarpkaya T.A critical review of the intrinsic nature of vortex-induced vibrations[J].Journal of Fluids and Structures,.19:389-447. 2004

[12]Govardhan R,Williamson C H K.Modes of vortex formation and frequency response of a freely vibrating cylinder[J].Journal of Fluid Mechanics.420:85-130. 2000